applied sciences

MDPI

Article

Evaluating the Quality of Reinforced Concrete Electric Railway Poles by Thermal Nondestructive Testing

Dmitry Valeryevich Sannikov [1], Alexander Sergeevich Kolevatov [1], Vladimir Platonovich Vavilov [1,2,*] and Marina Valeryevna Kuimova [1]

[1] School of Nondestructive Testing and Safety, Tomsk Polytechnic University, Lenin Av., 30, 634050 Tomsk, Russia; sanndv72@gmail.com (D.V.S.); shiryaev@tpu.ru (A.S.K.); kuimova@tpu.ru (M.V.K.)

[2] Department of Theoretical and Computational Mechanics, Tomsk State University, Lenin Av., 36, 634050 Tomsk, Russia

* Correspondence: vavilov@tpu.ru

Received: 11 December 2017; Accepted: 24 January 2018; Published: 1 February 2018

Abstract: Thermal nondestructive testing can be used to inspect reinforced concrete supports that are widely used in various industries. Corrosion damage is a typical defect found in these supports. Corrosion usually starts as a separation between the concrete and the steel rebar. Damage is exacerbated by pressure that is caused by the formation of corrosion products. The most logical method for using IR to detect corrosion or a disbond would be to heat up the rebar by resistive or inductive heating. In both cases, monitoring the dynamic temperature distributions on the pole allows for the evaluation of reinforcement quality. The thermal properties of steel, concrete, air, and corrosion products differ greatly. The magnitude of temperature anomalies and their behavior over time depend on the presence of corrosion products, air gaps, and the quality of contact between rebar and concrete.

Keywords: thermal testing; electric railway pole; inductive heating; numerical modeling

1. Introduction

In the inspection of reinforced concrete, a combination of induction heating and IR thermography was first suggested by Hillemeier et al. in 1982 [1]. General applications of this inspection technique were summarized by Maierhofer et al. [2]. Kobayashi and Banthia focused on the detection of corrosion by applying induction heating [3]. Milovanović et al. demonstrated that external optical stimulation of reinforcement in concrete enables detection of 10-cm structural elements in concrete at depths up to 7 cm [4]. Smaller thermal anomalies, such as 2 × 2 cm, can be detected up to a depth of about 4 cm [5]. Szymanic et al. described the use of microwave heating in the detection of rebars in concrete with a depth limit of about 2 cm [6].

This study covers the development of a thermal nondestructive testing (TNDT) technique for inspecting reinforced concrete supports of several types, such as overhead line poles, pipes, beams, pilings, etc., which are widely used in various industries, and in both the manufacturing and operation stages [7–9]. Historically, Russian railways represent one of the most important industrial areas in the country. It is worth mentioning that over 80% of cargo in Russia is being transported by means of railways (not counting the pipeline transport) [10]. Uncontrolled damage and full destruction of electrical supports may cause financial losses and even casualties, particularly in densely populated areas. Therefore, research intended to enhance the reliability of railway overhead lines is of a high priority in Russia, being supported by the corresponding federal directive documents. The mass electrification of Russian railways started in the 1980s. The lifetime of reinforced concrete poles is

assumed to be about 50 years, hence, in the near future, efficient inspection techniques to evaluate the quality of supports will become increasingly important.

Some poles may reveal an essential loss of their mechanical strength much earlier than within their normative lifetime. This may be conditioned by either poor workmanship or some ambient factors. Pole damage often starts in underground sections of supports, where corrosion appears because of varying soil moisture and high mechanical stresses. Corrosion damage is related to cracks that appear in concrete boundary layers adjacent to steel rebars because of enhanced pressure rendered by corrosion products. It is important to note that corrosion defects are located under the concrete surface layer and often hidden in the soil, thus are visually undetectable.

Figure 1 shows a scheme of an electric railway pole and typical corrosion defects that appear at a pre-failure period of operation. The most dangerous is corrosion damage, which appears in underground pole sections (Figure 1b).

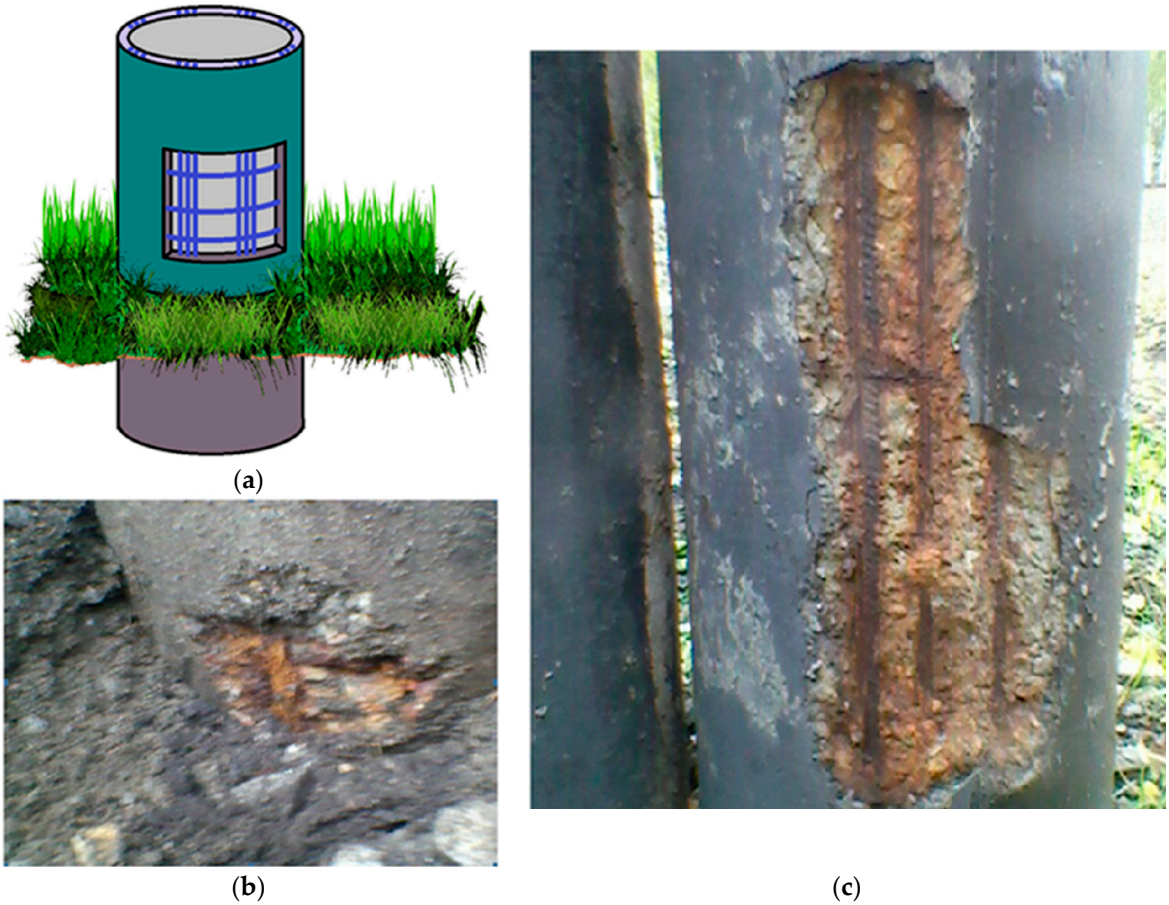

(**a**) (**b**) (**c**)

Figure 1. (**a**) Electric railway pole scheme; (**b**,**c**) and examples of corrosion damage.

A number of nondestructive testing (NDT) techniques have been applied to detect early corrosion in electric railway poles. They differ by sensitivity and test productivity but can hardly be applied to the evaluation of pole wear. The most usable ultrasonic inspection technique evaluates the strength of concrete by measuring ultrasound velocity in different directions or recording acoustic emission signals. Another ultrasonic test method involves the analysis of resonance features of the reinforcement. Both techniques are predominantly applicable for inspecting concrete surface layers and often require the use of special references.

One more inspection technique involves electromagnetic (induction) heating of a pole to locate reinforcement in concrete, but this does not help with the evaluation of residual reinforcement thickness. Classical TNDT based on surface heating of test objects seems to be inappropriate in the inspection of

concrete poles because of the considerable pole thickness and low thermal conductivity of concrete with regard to highly conductive steel. Alternatively, performing heating within internal cavities that are present in some types of poles is practically difficult. The use of solar heating for detecting damaged concrete in electric railway poles was reported elsewhere [11], but such a technique obviously cannot ensure high test reliability because of variable and low-power heating and the presence of multiple sources of thermal noise.

2. Inspection Schemes

The authors have suggested the stimulation of hidden metallic rebars by applying electric current or inductive heating. In both cases, the infrared (IR) thermographic monitoring of dynamic temperature distributions on the external bottom section of a pole allows for evaluating the quality of reinforcement. Since steel, concrete, air, and corrosion products differ by their thermal properties, significant test parameters, such as magnitude of temperature anomalies and their behavior over time, depend on the presence of corrosion products and the quality of contact between rebars and concrete. Both power and duration of electric pulses should be optimized to ensure detectable surface temperature signals.

There are four test configurations enabling the internal stimulation of rebars. In the first scheme, a source of electric current 5 is directly connected to rebars 2 via contact clamps 6 (Figure 2). Figure 3 shows the use of electrodes 7 placed on the surface of concrete without direct access to rebars. The third test configuration uses the natural grounding of concrete poles that are deeply buried in soil. In this case, one conductor is connected to a natural or artificial earth electrode 8 (Figure 4). However, the authors' practical experience has shown that the most effective technique is inductive stimulation of reinforcement (Figure 5) using high-frequency inductors 10 allowing contactless heating of metallic rebars inside concrete poles.

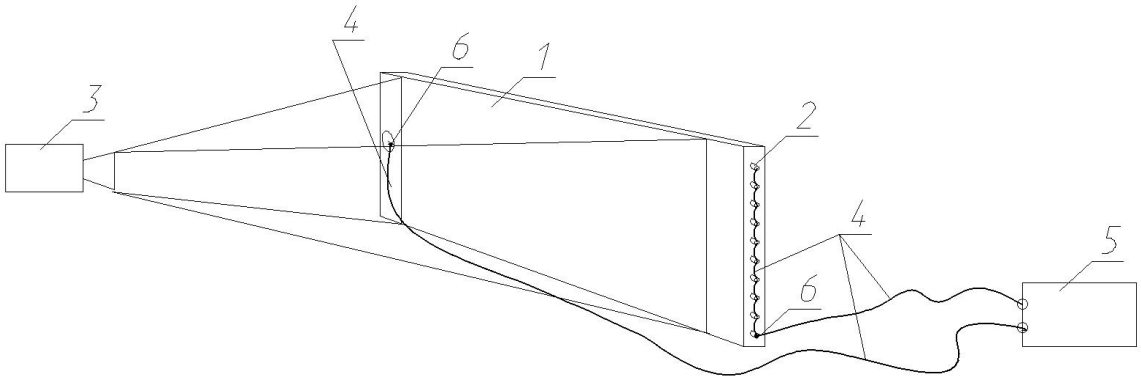

Figure 2. Direct connection of current source to reinforcement: (1—test object, 2—rebars, 3—IR imager, 4—cables, 5—current source, 6—contact clamps).

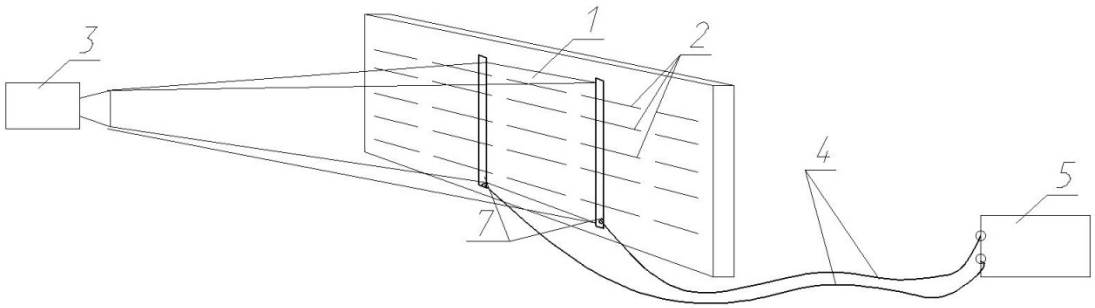

Figure 3. Using surface electrodes for heating rebars: (1—test object, 2—rebars, 3—IR imager, 4—cables, 5—current source, 7—surface electrodes).

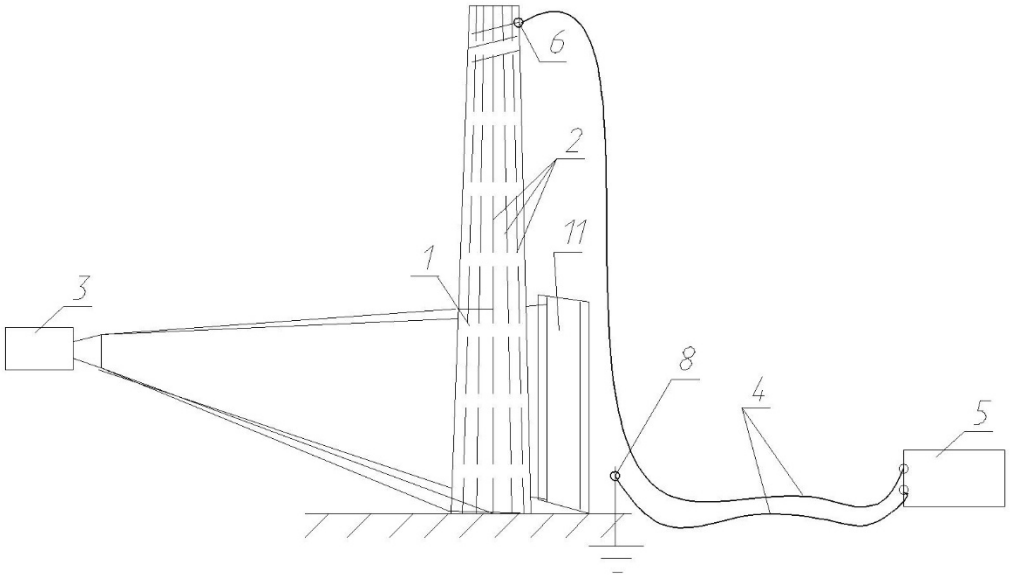

Figure 4. TNDT by using pole natural grounding and earth electrode: (1—test object, 2—rebars, 3—IR imager, 4—cables, 5—current source, 6—contact clamps, 8—natural/artificial earth electrode, 11—IR mirror).

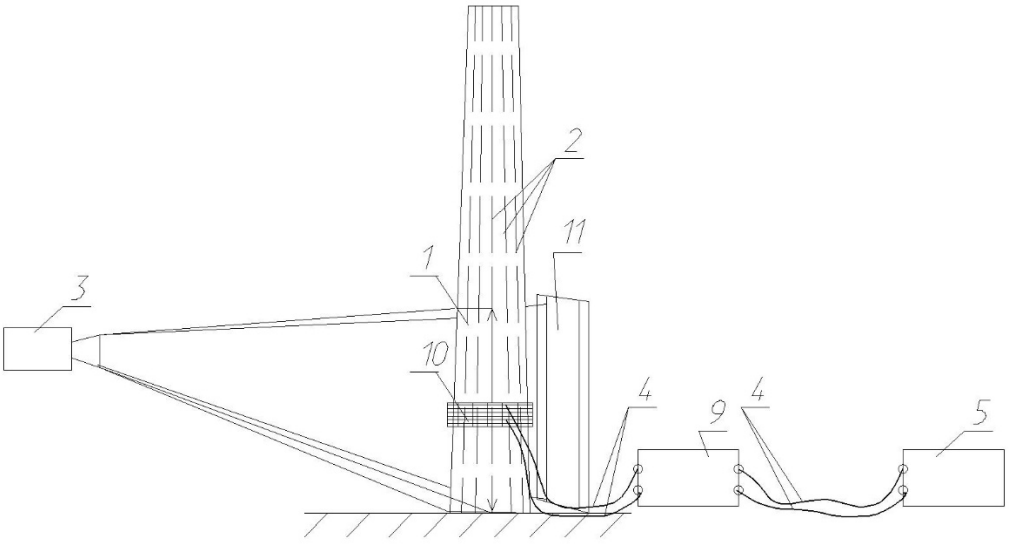

Figure 5. TNDT of electric railway poles by using inductive heating: (1—test object, 2—rebars, 3—IR imager, 4—cables, 5—current source, 9—high-frequency current transducer, 10—high-frequency inductor, 11—IR mirror).

Below we describe general principles and a step-by-step procedure of TNDT of railway electric poles by using inductive heating.

The inspection is performed by using at least one IR camera 1 (Figure 5). The inspection area can be expanded by using additional IR cameras or IR mirrors 11 made of materials with high reflectivity in the IR spectral band (for example, polished aluminum, etc.). A scheme of electric energy supply intended for rebar stimulation should be chosen taking into account the configuration and mass of test objects. Stimulation time and power are to be optimized by modeling particular test cases. Note that, by delivering a maximal heating power, one must avoid material damage accompanied by the appearance of burns and slags.

Synchronously with turning on a stimulation source, one starts recording a sequence of IR thermograms that reflects the evolution of pole surface temperature over time. Note that most of the thermal signals appropriate for further evaluation take place at a cooling stage when hidden defects can be detected by their specific temperature patterns on the inspected surface. By analyzing IR images, a thermographer is to outline areas with rebars and detect possible hidden defects, whose identification strongly depends on thermographer's experience. It has been found that an additional detection criterion, along with defect pattern amplitude and shape, is a rate of temperature variations in suspicious areas, i.e., the corresponding temperature derivatives.

The efficiency of the above test procedure depends on how uniform the heating of rebars is. This can be achieved by: (1) using transverse reinforcement (if available); (2) binding reinforcement with additional wires; (3) using grounding elements or special surface electrodes.

3. Modeling Test Cases

3.1. Inductive Heating

We are dealing with a 3D heat conduction problem for a non-adiabatic solid body with internal heat sources. The cylindrical geometry of a pole (Figure 6a) was replaced with a 3D Cartesian model shown in Figure 6b and numerically solved by using the ThermoSource software from Tomsk Polytechnic University (Figure 6c). The model simulates a 55 mm thick pole shell made of reinforced concrete (pole type SK8 by the Russian nomenclature). It is worth noting that in real poles, plenty of rebar bunches each including four 5 mm diameter steel rebars are regularly placed within a pole, as shown in Figure 6a. Each rebar bunch was simulated as a parallelepiped-like defect (cross section: 20 × 5 mm) and placed at depths of 10 and 20 mm from the external pole surface, and high-frequency powerful induction heating was simulated as energy discharge in a rebar (released power 10 MW/m^3, heating duration 20 s). The mathematical formulation of such TNDT problems was thoroughly discussed elsewhere [12,13]. Three characteristic areas are specified on the pole surface: a defect-free area (area 1 in Figure 6c), diminution of the rebar cross section by 25% (area 2), and the same rebar thinning but additionally accompanied with a 1 mm thick air-filled delamination (area 3). The latter defect is to simulate the practical situations, where the process of corrosion wear is accompanied by corrosion products that appear between concrete and reinforcement and provide pressure on the adjacent concrete, thus causing voids and cavities.

Two IR thermograms taken at 60 and 120 s are shown in Figure 7 to demonstrate that, over defect-free areas, the surface excess temperature ΔT reaches 8 °C (at 120 s if the defect depth is 10 mm); the rebar thinning results in a weak decrease of surface temperature because of the lower released energy while a significant temperature decrease occurs over the air-filled delamination because of its high thermal resistance. Temperature evolutions at three characteristic points (see Figure 7) in time (τ) are presented in Figure 8. Similarly to diffusivity measurement by using the known Parker technique, the fronts of temperature signals in Figure 8 depend on material thickness and thermal properties. This is also illustrated by Figure 9, where steel rebars are located at a depth of 20 mm. The thicker concrete layer diminishes both the excess surface temperature (down to 3 °C) and the rate of the temperature change.

The same dependencies are shown in Figure 9 for the case where steel rebars are located at a depth of 20 mm. The thicker concrete layer diminishes the surface temperature up to 3 °C and makes the rate of change in temperature slower.

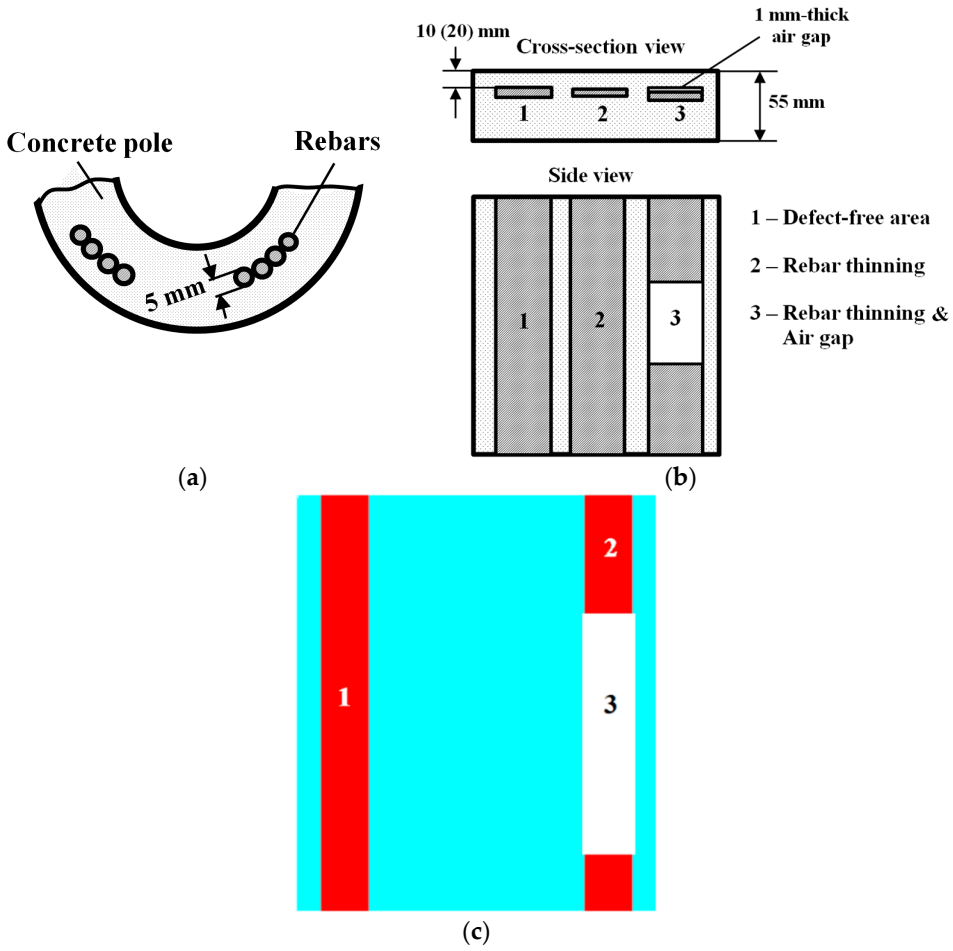

Figure 6. Railway pole 3D numerical model (wall thickness 55 mm, 5 mm diameter steel rebars at 10 (or 20) mm depth, 1—defect-free case, 2—defective case, rebar cross section diminished by 25%, 3—same as (2), additional 1 mm–thick air-filled delamination): (**a**) pole scheme; (**b**) Cartesian model; (**c**) ThermoSource software model, two rebars shown).

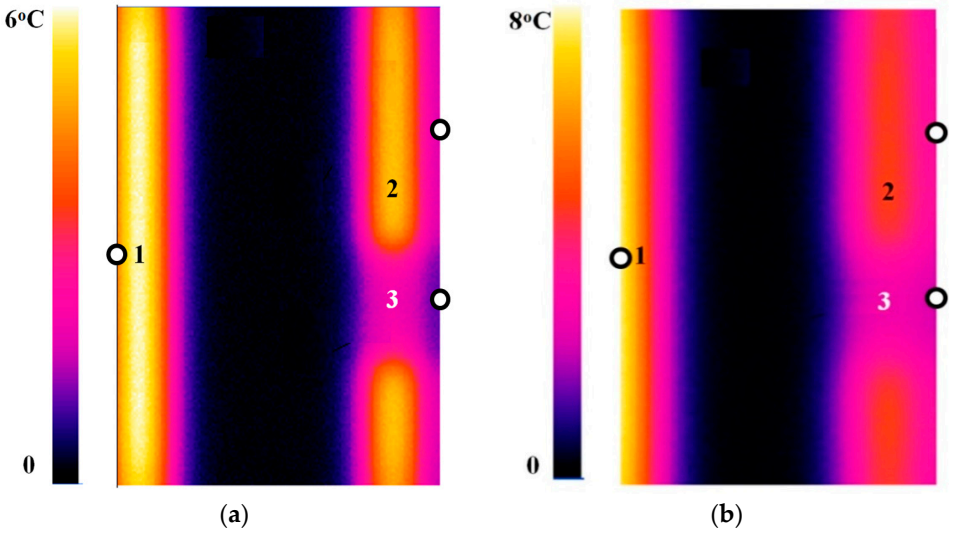

Figure 7. Synthetic IR thermograms of railway pole at 60 s (**a**) and 120 s (**b**) (model in Figure 6, reinforcement depth 10 mm, released power 10 MW/m^3, inductive heating duration 20 s).

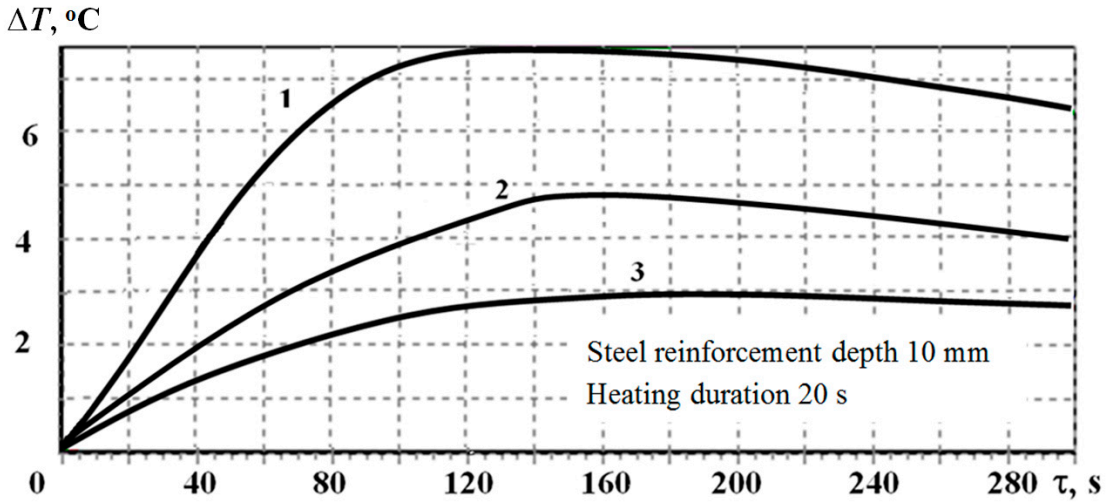

Figure 8. Temperature signal (ΔT) vs. time (τ) in the case of inductive heating at some characteristic surface points (model in Figure 6, steel reinforcement at 10 mm depth, points of interest shown in Figure 7, 1—defect-free case, 2—defective case, reinforcement cross section diminished by 25%, 3—same as (2) but additional 1 mm thick air-filled delamination).

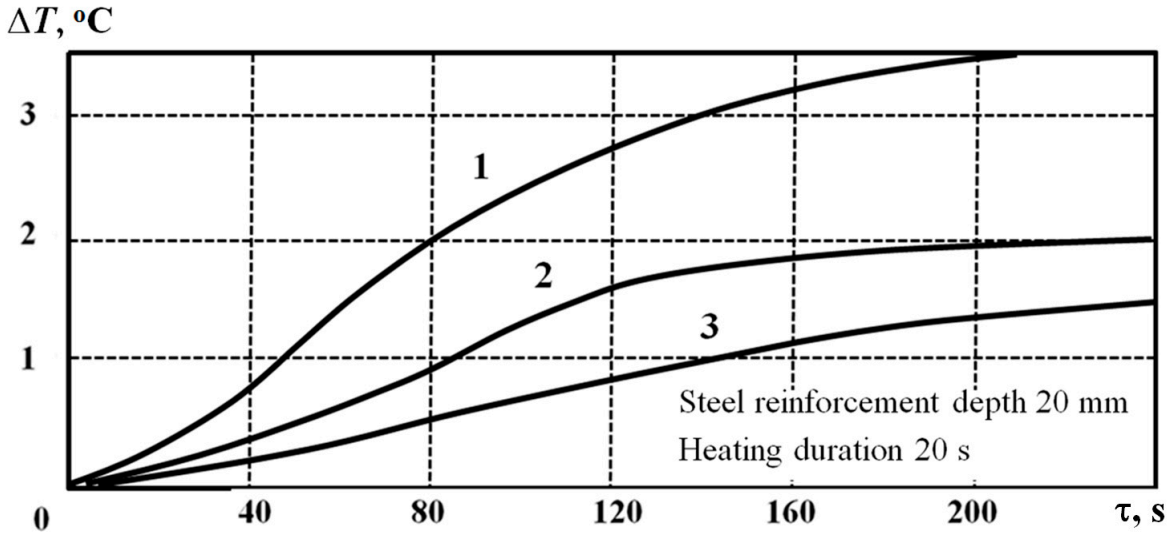

Figure 9. Temperature signal (ΔT) vs. time (τ) in the case of inductive heating at some characteristic surface points (model in Figure 6, steel reinforcement at 20 mm depth, points of interest shown in Figure 7, 1—defect-free case, 2—defective case, reinforcement cross section diminished by 25%, 3—same as (2) but additional 1 mm thick air-filled delamination).

3.2. Heating with Electric Current

Mathematically, heating with an electric current can be reduced to the same 3D heat conduction problem of heating a body by internal heat sources, as described above. In practice, electric current stimulation provides lower power release (400 W per linear meter of pole in our case) and thus should operate for a longer time (10 min) to ensure detectable temperature signals. Figure 10 shows synthetic IR images of dynamic temperature distributions. The images consist of two sections: the upper half-image is related to the above-ground section of the pole, while the bottom half-image exhibits the temperature distributions on the pole section buried in moistened soil. Rebar damage has been modeled by 20% rebar cross section thinning separated from the concrete surface layer by a 1 mm thick air gap. Defect-free reinforcement is characterized by excess temperature of about 10 °C (Figure 10a),

while the presence of an air gap diminishes surface temperature signals in the above-ground bottom section of the pole by about 3–4 °C (Figure 10b).

Figures 11 and 12 present graphs of both surface temperature and temperature time derivatives for three test cases, respectively (see the figure caption). Qualitatively, the temperature evolutions look similar to those in Figures 8 and 9, and the temperature values conditioned by total released energy are close to the case of inductive heating. The modeling shows that the temperature maximums appear at about the same times over rebars of different thickness but a 1 mm thick air gap in a pole with a 55 mm thick wall diminishes the temperature evolution rate up to 3-fold with regard to non-defect areas (Figure 12). Hence, variations in the temperature evolution rate (temperature derivative) can be used for identifying air gaps. However, the use of this phenomenon in practice may require smoothing experimental temperature evolutions because taking derivatives tends to enhance high-frequency noise.

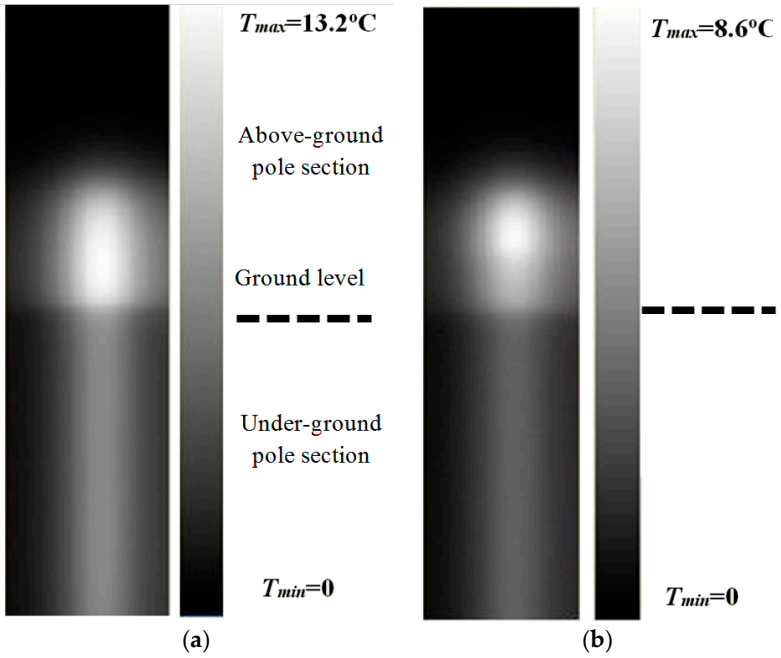

Figure 10. Synthetic temperature distributions in case of non-defective (**a**) and defective (**b**) reinforcement.

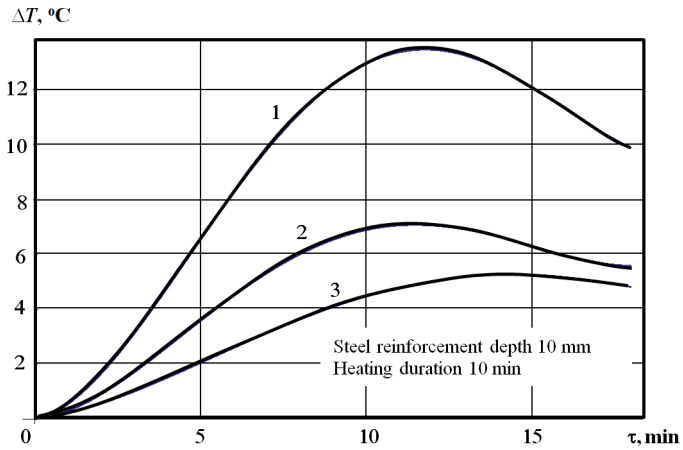

Figure 11. Temperature signal (ΔT) vs. time (τ) in the case of heating with electric current: 1—defect-free reinforcement, 2—rebar cross section diminished by 20%, 3—rebar cross section diminished by 20% with additional 1 mm thick air gap.

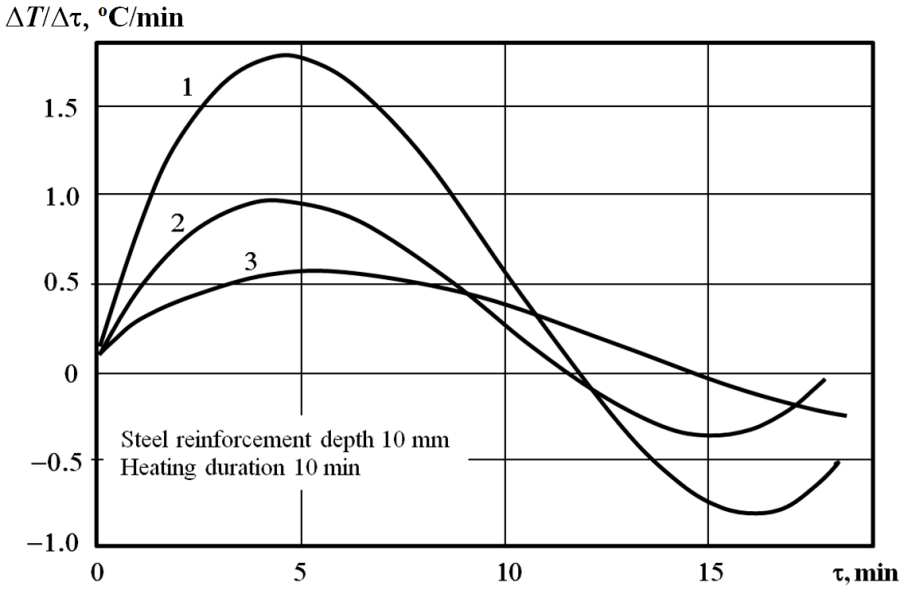

Figure 12. Temperature derivative ($\Delta T/\Delta\tau$) vs. time (τ) (see caption for Figure 11).

4. Experimentation and Discussion

The authors' practical experience suggested that these testing techniques can be applied to the inspection of in-field railway electric poles. If inspection is performed by the scheme of Figure 4, i.e., by using natural grounding, one can avoid digging out an underground pole section due to the temperature distribution at the ground level allowing for the evaluation of the electric current flowing down through rebars. The corresponding surface temperature pattern reflects the severity and localization of damage in the pole underground section. In its turn, the monitoring of a 1–2 m long above-ground pole section allows for the detection of such defects as thinning of rebar cross-section, the presence of corrosion products, concrete delaminations, etc. To simultaneously view the rear side of the poles during a single heating cycle, one can use, as mentioned above, IR mirrors or additional IR cameras.

In TNDT, test results can often be improved by increasing heating power. In order to avoid damaging a pole protective layer by using additional electrodes, it is convenient to apply non-contact inductive heating by the scheme of Figure 5 in a narrow circular area on the pole surface. By moving both the heater and the IR camera, one can observe pole temperature response under constant heating conditions. Since the thermal conductivity of concrete is relatively low, an optimal inspection area is located several centimeters from the heated zone, thus being unaffected by powerful thermal radiation from the heating zone. A similar procedure was used by Green in the 1970s to test quality of nuclear fuel elements [14]. Theoretical aspects of line heating were discussed elsewhere [12], and its practical implementation was done in the inspection of boiler sections [15].

Experimental section of this study was performed on the Transsiberian railway (JSCo "Russian Railways") by using a pilot experimental setup. We have checked 14 operating poles with a pre-stressed steel reinforcement of the SK type (same as simulated) by using three NDT methods: IR thermographic, ultrasonic, and vibroacoustic.

Thermal stimulation of poles was accomplished by means of an inductive heater powered from an autonomous gasoline generator that was mounted on a truck. The inductor coil was moving up along a test pole with velocity from 5 to 10 mm/s by using a special lifting device (see Figure 13a). Bottom sections of the poles under test were dug out by about 0.5 m to allow their direct IR surveying. Each pole area was inductively heated for about 20 s, the same as in the modeling.

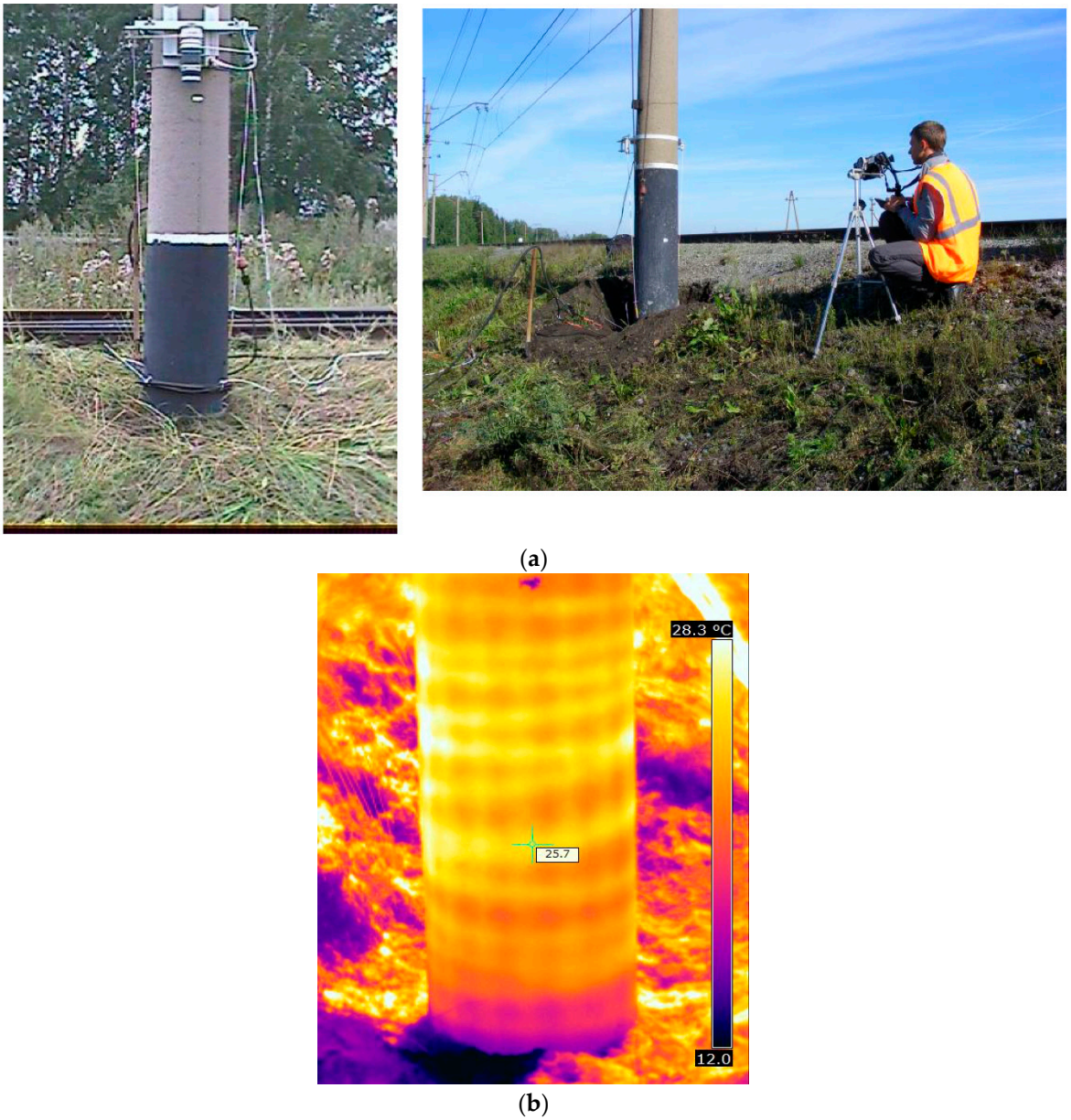

(**a**)

(**b**)

Figure 13. (**a**) Inspecting quality of electric railway poles: test site view; (**b**) typical IR thermogram.

Thermal NDT was accomplished on a 1 m long pole area including a 0.5 m long underground section. The inspected area was outlined with aluminum markers that were visible in both IR and visual images. Pole surface temperature was monitored on a dry sunny day (ambient temperature 25–30 °C) by using a FLIR P60 IR camera mounted on a tripod (Figure 13a). A typical IR thermogram of a defect-free pole is presented in Figure 13b to clearly show the warmed-up subsurface reinforcement.

Recorded images were processed to produce synthetic images containing extreme values of parameters chosen as significant—for example, images of maximal temperatures achieved during the whole thermal process (the so-called "maxigrams"). Figure 14a shows a defect-free pole section located above the ground level. It is clearly seen that the surface 'footprints' of the reinforcement are regularly located and characterized by the same excess temperature in the range from 7 to 8 °C. In the case of a damaged pole (Figure 14b), the corresponding maxigram shows a distinct area of decreased temperature that apparently corresponds to debonding between the concrete and the reinforcement.

In defect areas, the excess temperature dropped by about 4–5 °C, being in the same range of magnitude as predicted by the simulation.

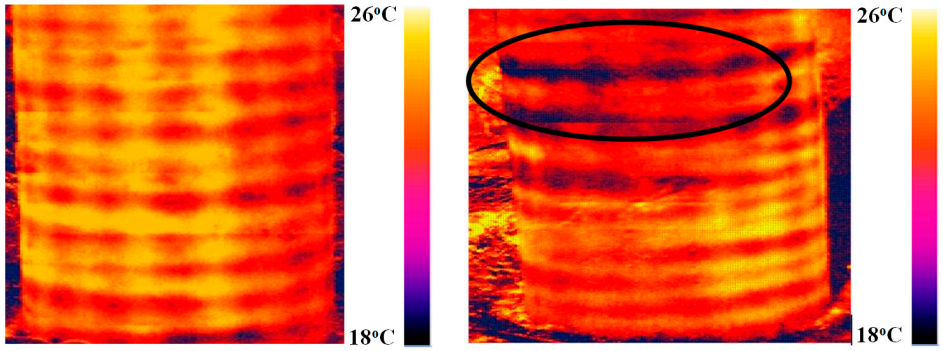

Figure 14. Maxigrams of a defect-free (**a**) and damaged (**b**) pole (pole section above ground level).

In general, it has been found that both types of reinforcement, namely, circumferential and longitudinal, can be clearly detected 20 cm above the ground level, and the temperature contrast has been good enough to reliably identify the localization of reinforcement.

Similar results appeared when we inspected the below-ground pole sections (see the example of a tested pole in Figure 15a). In this case, the maxigram revealed some electric corrosion. In particular, no indications of circumferential reinforcement were found in the pole underground sections (Figure 15b). In this case, except for a general decay of temperature on the pole surface, the temperature vs. time curves revealed a decrease in temperature variation rate by 2–4 times with regard to defect-free areas (Figure 16). In conjunction with a delayed temperature maximum appearing at about 170 s, this, according to the theoretical predictions, suggests the presence of hidden delaminations between the concrete and the reinforcement.

Visual inspection of the underground pole section revealed some cracks and weak traces of corrosion products. The results of ultrasonic and vibroacoustic tests were also beyond the corresponding norms accepted in Russia, thus confirming the IR thermographic findings.

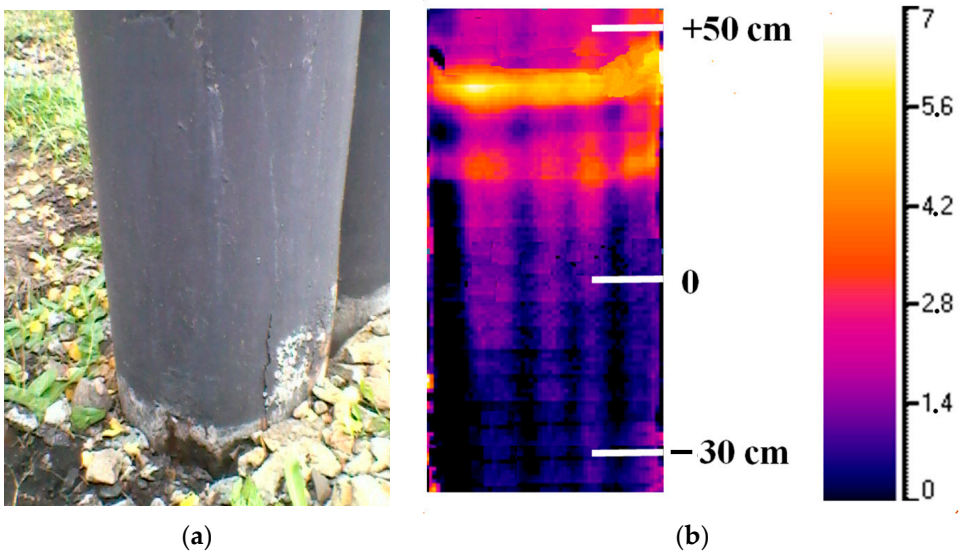

Figure 15. Photo (**a**) and maxigram (**b**) of a damaged pole (pole section below ground level).

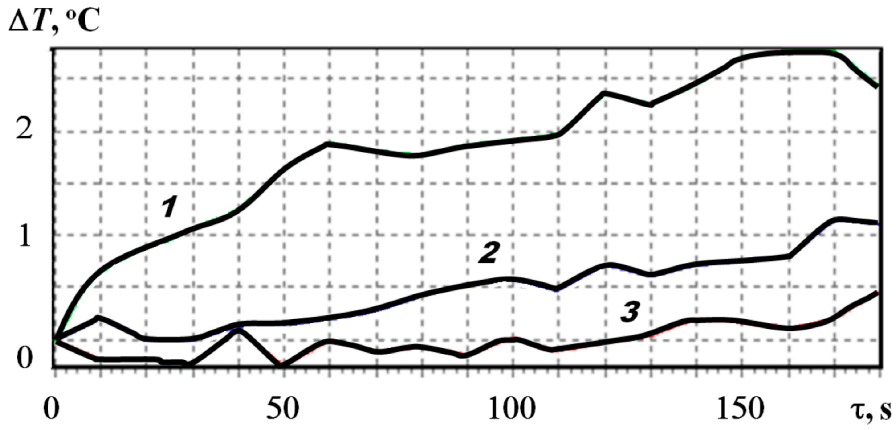

Figure 16. Experimental temperature profiles at the ground level: pole excess temperature vs. time (1—+50 cm, 2—0 cm, 3—−30 cm).

Following the results of IR thermographic surveys, the two inspected poles were replaced. The presence of electric corrosion damage was confirmed by a mechanical destruction test. In parallel, the acceptable quality of other inspected poles was confirmed by comparing the results of ultrasonic and vibroacoustic testing (these results will be discussed in a forthcoming paper).

5. Conclusions

In this study, we have used the known techniques of IR thermographic nondestructive testing and the scanning heating of cylindrical objects. However, these techniques are innovatively applied to a new class of test objects. Also, the implementation of heating devices and data processing using a concept of maxigrams is novel.

TNDT has been used for performing evaluations of reinforced concrete poles on operating railways. This technique is safe for personnel and fully nondestructive since the excess pole temperature does not exceed 15 °C.

IR imaging allows the visualization of both longitudinal and circumferential rebar reinforcement, and whether corrosion has caused a separation between the rebar and the concrete. By heating poles inductively (released power: about 10 MW/m^3) or applying electric current (up to 400 W per linear meter of a pole), surface temperature signals in defect areas may reach 3–10 °C depending on reinforcement depth, as well as a grade of rebar thinning and presence of corrosion products characterized by high thermal resistance. The same defects diminish the rate of temperature changes (temperature derivative) by 2–4-fold, which can be used for defect identification.

It has been experimentally determined that galvanic corrosion in concrete pole reinforcement can be detected in pole sections located higher than 20 cm above the ground level. To evaluate underground sections, a pole should be unearthed for about 20–30 cm below the ground level, although in some cases it is not necessary. It is worth mentioning that, until now, corrosion damage could only be detected just prior to the failure of a pole. However, this technique can detect damage well before failure.

TNDT surveys can detect reinforcement displacement and predict the residual strength of poles by analyzing concrete cracking in the near-ground pole section. This is a goal of the ongoing research.

Acknowledgments: This work was supported by a Russian Scientific Foundation grant #17-19-01047 (3D numerical modeling) and in part by a State Order of the Russian Ministry of Higher Education for 2017–2019, NIR #9.5966.2017/BY (experimental implementation).

Author Contributions: Dmitry Valeryevich Sannikov conceived and designed the experiments. Alexander Sergeevich Kolevatov performed the experiments. Vladimir Platonovich Vavilov did the numerical modeling of defect situations. Marina Valeryevna Kuimova wrote the paper.

Conflicts of Interest: The authors declare no conflict of interest.

References

1. Hillemeier, B. Method of Determining the Location, Orientation and Pattern of Reinforcing Members in Reinforced Concrete. U.S. Patent 4309610, 5 January 1982.
2. Maierhofer, C.; Reinhardt, H.W.; Dobmann, G. (Eds.) *Non-Destructive Evaluation of Reinforced Concrete Structures*; Woodhead Publishing CRC Press: Cambridge, UK, 2010; 624p, ISBN 978184569950.
3. Kobayashi, K.; Banthia, N. Corrosion detection in reinforced concrete by using induction heating and infrared thermography. *J. Civ. Struct. Health Monit.* **2011**, *1*, 25–35. [CrossRef]
4. Milovanović, B. Detecting defects in reinforced concrete using the method of infrared thermography. *CrSNDT J.* **2013**, *3*, 3–13.
5. Cannard, H.; Mahrez, M.; Perrin, T.; Muzet, V.; Prybyla, D.; Brachelet, F. The use of infrared thermography for defects detection on reinforced concrete bridges. In Proceedings of the 12th Quantitative InfraRed Thermography Conference, Bordeaux, France, 7–11 July 2014. [CrossRef]
6. Szymanik, B.; Karol-Frankowski, P.; Czady, T.; Chelliah, C. Detection and inspection of steel bars in reinforced concrete structures using active infrared thermography with microwave excitation and eddy current sensors. *Sensors* **2016**, *16*, 234. [CrossRef] [PubMed]
7. American Society of Civil Engineers, USA. *Guide for the Design and Use of Concrete Poles*; American Society of Civil Engineers: Reston, VA, USA, 1987; 53p, ISBN 0-87262-596-6.
8. Tsunemoto, M.; Shimizu, M.; Kondo, Y.; Kudo, T.; Ueda, H.; Ijima, T. Replacement criteria for concrete catenary poles. *Q. Rep. RTRI* **2017**, *58*, 270–276. [CrossRef]
9. Ausgrid Network Standard NS145. Pole Inspection and Treatment Procedures. Available online: www.ausgrid.com.au/-/media/Files/Network/Documents/NS-and-NUS/NS145.pdf (accessed on 3 August 2017).
10. Russian Federation Government Analytical Centre. *Bulletin of the Socio-Economic Crisis in Russia: Dynamics of Cargo Transportation in Russia*; Russian Federation Government Analytical Centre: Moscow, Russia, 2015; 24p. (In Russian)
11. Frumuselu, D.; Radu, C. IR thermography applied to ground-level reinforced concrete constructions belonging to electricity networks. *Insight* **1998**, *40*, 501–504.
12. Vavilov, V.; Taylor, R. Theoretical and practical aspects of the thermal NDT of bonded structures. In *Research Techniques in NDT*; Sharpe, R., Ed.; Academic Press: London, UK, 1982; Volume 5, pp. 239–280, ISBN 0-12-639055-X.
13. Vavilov, V.P.; Burleigh, D.D. Review of pulsed thermal NDT: Physical principles, theory and data processing. *NDT E Int.* **2015**, *73*, 28–52. [CrossRef]
14. Green, D.R. Principles and applications of emittance-independent infrared nondestructive testing. *Appl. Opt.* **1968**, *7*, 1796–1805. [CrossRef] [PubMed]
15. Woolard, D.; Cramer, K. The thermal photocopier: A new concept for thermal NDT. *Proc. SPIE* **2004**, *5405*, 366–373. [CrossRef]